IEEE Journal of Microwaves

Received 21 August 2023; revised 5 November 2023 and 17 December 2023; accepted 17 January 2024. Date of publication 9 February 2024; date of current version 9 April 2024.

Digital Object Identifier 10.1109/JMW.2024.3356308

Integrated Wideband Multiplexer Design for Multiple-Use SATCOM/Terrestrial Terminals

CHAD BARTLETT [1] (Member, IEEE), MICHAEL HÖFT [1] (Senior Member, IEEE), AND UWE ROSENBERG [2] (Life Senior Member, IEEE)

(Regular Paper)

[1]Institute of Electrical and Information Engineering, University of Kiel, SH 24143 Kiel, Germany
[2]Consultant U. Rosenberg, 27711 Osterholz-Scharmbeck, Germany

CORRESPONDING AUTHOR: Chad Bartlett (e-mail: cbartlett@ieee.org).

This work was supported by the Schleswig-Holstein State Open-Access publication funding programme.

ABSTRACT A novel wideband multiplexer is introduced as a communications equipment solution in order to provide simultaneous operation of satellite and terrestrial services in the dedicated *K*/*Ka* frequency bands (passbands ranging from 19.5 GHz to 30.5 GHz). Advanced RF filtering techniques are applied in order to accommodate a compact multiplexer design while maintaining low insertion loss and high rejection demands up to 33 GHz. Due to the overall wide bandwidth and the demanding requirements for the assigned three operational bands, different filter types have been employed. Thus, the multiplexer considers the combination of filters with rectangular, evanescent combline, and conductor-loaded resonator types. The multiplexer relies on the direct branching approach, i.e., all filters are connected to a central (star-junction) waveguide branching region. This region exhibits a reduced waveguide size to suppress interference by higher order modes. For a verification of the approach, WR34 waveguide interfaces have been considered at all ports for prototype design, however, the design can be well adapted for integrated equipment solutions with associated direct interfaces. Accurate coincidence of analyzed and measured performance of the prototype demonstrates the validity of the special approach. Moreover, additional simulations are provided as an outline for terminals with specific industry demands.

INDEX TERMS Filter design, high-precision milling, high-throughput satellites (HTS), multi-band, multi-use terminals, multiplexers, Satcom, satellite communication, star junction, wideband filters.

I. INTRODUCTION

Advanced communication equipment is required to support future multi-use applications such as simultaneous satellite and terrestrial services [1]. Integrated systems such as these require complex solutions that are capable of combining modern high-throughput satellite (HTS) services – which rely on Frequency Division Duplex (FDD) and operate at frequencies such as 20 GHz for downlink (DL) and 30 GHz for uplink (UL) – with state-of-the-art communication networks (i.e, 5G Enhanced Mobile Broadband (eMBB)), which are based on Time Division Duplex (TDD) and assigned broad frequency bands located around 25 GHz.

In this regard, highly stringent performance requirements necessitate the pioneering of new and unconventional solutions to unlock the potential of future HTS architectures and $\geq$5G/6G networks, and moreover, can help to unlock other desirable benefits or applications, such as highly miniaturized designs, effective smart-jamming counter measures, and integrated multiplexing/demultiplexing antennas [1], [2], [3], [4], [5]. One prerequisite of an equipment design providing the combined FDD and TDD services is a wideband multiplexer for the combination and separation of these frequency bands while feeding a common antenna. In general, many requirements for such wideband multiplexers must be considered, that being; low insertion loss, high inter-band isolation and high suppression of spurious signals. These considerations must all be met while conforming to requirements such as compact size, convenient interfacing, and integration within the equipment to accommodate overall low cost.

TABLE 1 ***K/Ka*-Band Multiplexer - Performance Demands**

	Satcom (Downlink)	Satcom (Uplink)	5/6G
Operational Band [GHz]	19.75 to 21.0	29.75 to 30.25	23.75 to 27.25
Insertion Loss [dB]	<1.0	<1.0	<1.0
Return Loss [dB]	>18	>18	>18
Rejection / Guard [dB]			
| 18.0 to 21.25 GHz	-	60	60
| 22.25 to 22.75 GHz	30	60	30
| 23.5 to 27.5 GHz	60	60	-
| 28.25 to 28.75 GHz	60	30	30
| 29.75 to 33.0 GHz	60	-	60
Temp. Range [°C]	-20 to +80		
Size [mm^3]	<100 x 100 x 10‡		
Mass [g]	<500		

‡Size for integrated design; prototype considers standard WR34 waveguide flanges (square 22.4 mm) for verification measurements

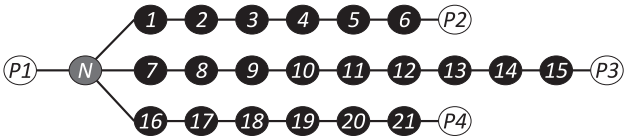

FIGURE 1. Topology of the multiplexer with a star junction. Resonating nodes are black, source/load nodes are white, and the grey node is a nonresonating star junction. Solid lines indicate the direct-coupling path.

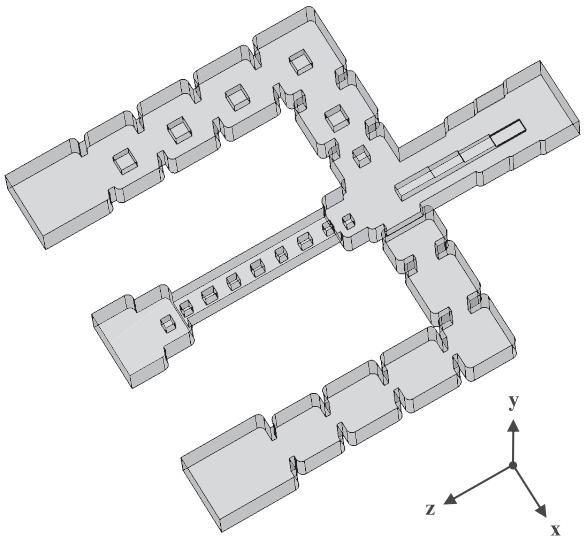

FIGURE 2. Perspective view of the proposed multiplexer concept utilizing various filter techniques to achieve wideband communications throughout the *K* and *Ka* band regions.

Although manifold-style multiplexers have been well defined in the literature ([6], [7], [8], [9], [10], [11], [12]) for both star- and manifold-coupled designs, the vast majority of designs are contrived for tightly-spaced narrowband channel selection and utilize a manifold coupling scheme to allow for the additional degree of freedom provided between each contiguous filter branch. Work in this field has spanned all the way to the terahertz region and across many technology platforms (e.g., [13], [14], [15]. However, on the consideration of wideband channels, it is common to see configurations that utilize lowpass filter techniques to allow for a wide lowpass response while the upper-ranged filter response is provided by a single bandpass or highpass filter [16], [17], [18]; in this scheme, the device often becomes limited to operate as a diplexer due to the frequency region of interest being covered by the combination of lowpass/highpass responses. Albeit, this operational limitation can be overcome by the clever routing of multiple diplexers and power dividers and can be used to achieve wideband operation - for example in [19] - but comes at the cost of size and optimal electrical performance.

Integrating multiple channels that are capable of wideband configurations and spanning multiple frequency bands – all within a compact housing – becomes highly challenging to design and can be very difficult to manage optimal multiplexing characteristics. Surveying the current literature, there seems to be no simple approach put forth for obtaining the high-performance requirements of multiband, wideband-channel multiplexers.

This work introduces a novel method for ascertaining very-wide operational multiplexer bandwidths (MUX FBW = 42%) and capable of covering multiple frequency bands with high isolation characteristics, all within a highly compact and easily manufacturable H-plane format, by utilizing the unique Q-factor and rejection characteristics provided by different cavity-filter types, in order to meet the stringent filtering requirements imposed by future HTS architectures that desire operation with integrated FDD and TDD communication methods. The proposed multiplexer design relies on three distinct waveguide filter types for the separate branch specifications, namely, direct-coupled rectangular cavities, evanescent combline resonators, and conductor-loaded resonators. Each of these filter branches is connected to a common junction, which provide connection to the common feed port of the multiplexer. For equipment integration, there is no need to consider standard waveguide interfaces at the ports, i.e., they can conveniently be adapted for optimal interconnections within the equipment [1], [20]. However, for the validation of the design approach, WR34 waveguide interfaces are considered for a prototype design at all ports. Due to this measurement scenario, a ridge waveguide transformer is considered as an interconnection means to the common-port. Accordingly, a prototype is fabricated and accurate coincidence of analyzed and measured responses of the multiplexer is demonstrated. To conclude this work, additional simulations are provided in a *Future Applications* section in order to demonstrate successful fulfilment of industry specifications for upcoming multiple-use Satcom/terrestrial terminals.

II. WIDEBAND MULTIPLEXER REQUIREMENTS AND FILTERING BRANCHES

Filter and multiplexer designs generally start with the evaluation of the appropriate filter functions and suitable filter types

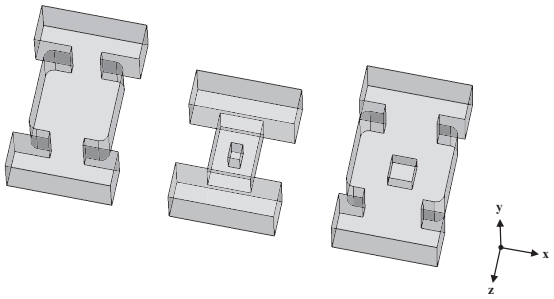

FIGURE 3. Sample vacuum-shell forms of each resonator type for demonstration of S-parameter characteristics in Fig. 4. From left to right: Rectangular cavity (RC), evanescent combline structure (CL), and conductor-loaded cavity (CDL).

TABLE 2 Typical Resonator Quality Factor of Resonators in the Proposed *K/Ka*-Band Multiplexer

	Rectangular Cavity	Combline Structure	Conductor-Loaded Cavity
$Q_{unloaded}$	2600	1250	2000

Effective conductivity is taken as 15.6 MS/m.

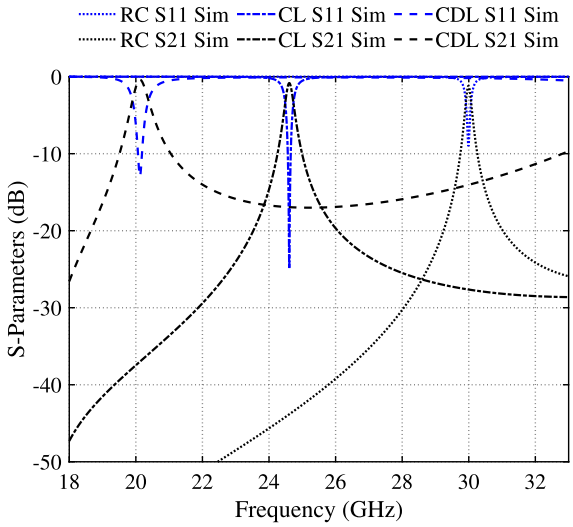

FIGURE 4. Simulated S-parameter characteristics of first-order resonator types specified in the system as shown in Fig. 3. Effective conductivity is taken as 15.6 MS/m.

to achieve given specifications. In the case of wideband multiplexer designs the initial assessment of the filter functions and suitable implementations of the individual filters is decisively important when considering the overall requirements, i.e., RF performance (incl. far band requirements), environmental conditions, mass, size and interfacing. Moreover, the filter types should provide suitable adaptation to the multiplexer design. Table 1 summarizes the specifications for the multi-use *K*/*Ka*-band wideband multiplexer where the distinct bands are designated for Satcom downlink, uplink, and 5/6G communication.

For meeting the stringent requirements such as low insertion loss and steep rejection characteristics, several approaches can be employed. For instance, the utilization of transmission zeros can improve the rejection and isolation characteristics while reducing the number of cavities that would generally be required in an all-pole design. A range of creative examples can be reviewed in work such as [21], [22], [23], [24], [25], [26], [27], [28]. However, these designs generally require cross-coupling techniques or extensive knowledge on techniques such as nonresonating modes or frequency-dependent couplings, and in the case of very wideband widths, still require a significant amount of resonators to achieve the desired passband characteristics. A traditional method would suggest to cascade a number of direct-coupled rectangular resonators with capacitive or inductive irises until the specifications for a suitable bandwidth and isolation is met. This all-pole method is well-known and explored in many articles throughout the literature in different technologies and configurations, [7], [10], [29], [30], [31], [32] are to mention but a few. In order to achieve multiple filter passbands over a very wide range however, we propose the use of several different filter types that follow a similar all-pole approach. In this manner, we specify the required frequency bands with filters that are capable of obtaining the required bandwidth and both the near and far out-of-band rejection characteristics that will allow for each branch to operate well isolated from one another and mitigate any interband interference [33], [34].

Based on the specifications outlined in Table 1, suitable filter functions and filter types are explored for the different branches. Commonly, multiplexer filter designs have to account for implementation (e.g., manufacturing tolerances) and technology/operational aspects (e.g., frequency offset over temperature). Consequently, basic filter assessments consider enlarged bandwidths to satisfy the final required performance for all operational conditions and the chosen technology/production method. For the filter designs of the required broadband multiplexer, the chosen bandwidths (equiripple return loss 20 dB) are 500 MHz larger than the operational bands (cf. Table 1). The additional consideration and study of these margins for the nearband rejection of each passband yields 6th-order filter characteristics for the Satcom downlink and uplink, and a 9th-order filter for the 5/6G branch, where the generalized Chebyshev coupling matrix entries correspond to $M_{S1} = M_{6L} = 1.002$, $M_{12} = M_{56} = 0.843$, $M_{23} = M_{45} = 0.611$, $M_{34} = 0.583$ and $M_{S1} = M_{9L} = 0.988$, $M_{12} = M_{89} = 0.817$, $M_{23} = M_{78} = 0.587$, $M_{34} = M_{67} = 0.548$, $M_{45} = M_{56} = 0.537$ for the initial 6th-order and 9th-order filters, respectively. These filters are then to be connected to a common (star) junction to realize the wideband multiplexer. A star-junction has been chosen in order to maintain an inherently small connection point and corporate-feed to the multiplexer's common port in an H-plane topology, where other feeding styles such as manifolds or power dividers can require large corporate-feed sections, additional spacing for splitters, or alter the feed orientations, which also can in turn limit the achievable out-of-band isolation, while E-plane topologies can create difficulties in milling/assembly of different waveguide types. Fig. 1 depicts the circuit topology of the proposed design. The continuing task is related to

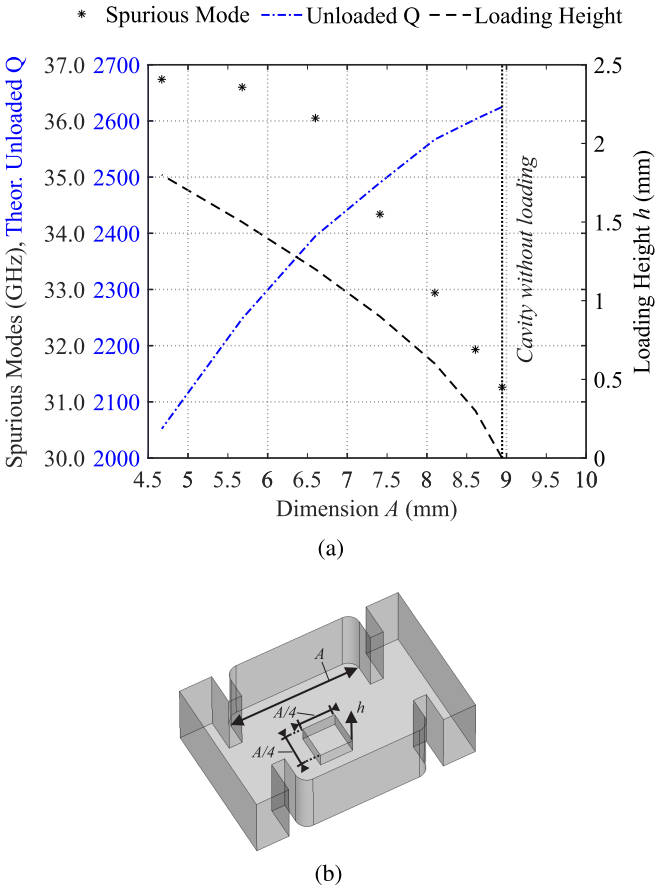

FIGURE 5. (a) Simulated investigation of the unloaded Q and next induced spurious mode of a conductor-loaded cavity with the center frequency held at 22 GHz. (a) variation of the principle cavity dimensions *A* and *h*, and (b) the simulated vacuum-shell of the cavity with WR34 waveguide dimensions. The irises are set for a length and width of 0.8 mm and 4.8 mm, respectively. Effective conductivity is taken as 15.6 MS/m.

the investigation of appropriate filter types, i.e., the basic resonator/cavity designs with associated coupling configurations. The evaluations aim at compromising overall RF performance and implementation aspects, related to unloaded Q, spurious mode performance, size and implementation capabilities. For instance, the requirements for the different branches exhibit significant differences in required bandwidths and spurious mode performance. Hence, the far out-of-band rejection specifications that are required above the respective passbands are critical for the two lower filters. Obviously, there would be no problem with far out-of-band requirements below the overall band due to the waveguide cut-off. Thus, the filter trade-offs for the different branch types must be considered for each of the consecutive branches.

The aim of low insertion loss filters is commonly accommodated by considering waveguide cavity types providing high unloaded Qs. In addition, it is well known, that the insertion loss is inversely proportional to the bandwidth. Thus, the unloaded Q becomes more important for the narrowband filters in multiplexer designs, when focusing on similar passband insertion losses. At the same time, the vital issue for multiplexer filter designs is the consideration of spurious mode control. Especially in case of broadband applications, higher-order modes of the lower channel filters may fall into or close to the multiplexer's higher frequency passbands. This could yield many difficulties or even make a design impossible. Moreover, there may also be strict far out-of-band rejection requirements above the highest channel that need to be satisfied.

As a prelude to the following discussion on individual filter branches, the general vacuum-shell layout of the goal (proposed design) is provided in Fig. 2 for reference.

The integrated approach starts with the initial filter designs for the three branches that will be interconnected between the four port junction and their respective output ports. WR34 has been selected specifically in order to utilize the full *Ka*-band from 22 GHz to 33 GHz, as well as below the recommended specification of 22 GHz, down to 18 GHz. This is of course possible due to the WR34 cutoff frequency being located at approximately 17.4 GHz, and the next higher-order mode cutoff appearing at approximately 34.7 GHz. Fig. 3 demonstrates the three types of resonators considered: direct-coupled rectangular cavity, evanescent combline resonator, and conductor-loaded resonator. Fig. 4 and Table 2 are provided as a general overview of the single cavity response and subsequent rejection characteristics.

Contrary to the modes in rectangular waveguide cavities, the field components in ridge waveguides cannot be obtained by a simple separation of the variables in the wave equation [10]. A more systematic approach can be followed from the study of resonators as demonstrated in the example of Fig. 5, where the resonant frequency of a cavity is held at 22 GHz, and a trade off of dimensions with respect to Q-factor and the next generated spurious modes is demonstrated. This approach can be followed for the initial design of useful cavities before optimization of filter dimensions and subsequent iris loading effects. The analysis of an empty cavity (cf. Fig. 5) yields the next higher spurious resonance mode at approximately 31.26 GHz, consequently, such a cavity design would be not suitable since this spurious resonance falls into the high rejection band. Moreover, it would (at least) significantly impair the multiplexer design, due to the close distance to the highest channel passband. Hence, special design considerations for the lower filter channel's resonators/cavities must be introduced to ascertain the final multiplexer design. This dedicated cavity design method focuses on compromising high unloaded Q of the resonance modes and sufficient frequency distance to the next higher spurious modes. It can also be noted that the conductor-loaded cavity types are an intermediate solution between waveguide and combline resonators; compromising special design demands as in the present case (e.g., unloaded Q, spurious performance, size).

Following the topology presented in Fig. 1, the filters branches are designed with the dedicated resonator types and formulated as shown in the indicative layout provided in Fig. 2.

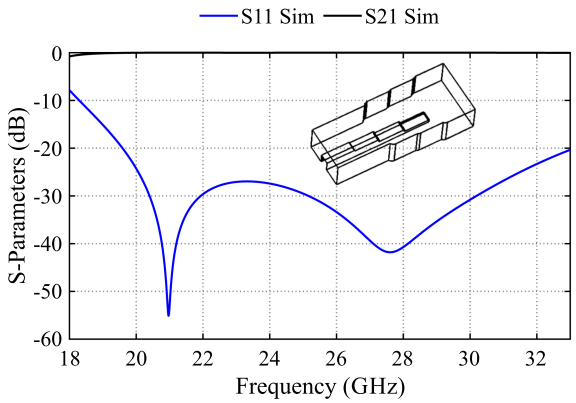

FIGURE 6. Simulated S-parameter characteristics of the single ridge waveguide transition at the input of the multiplexer's star junction.

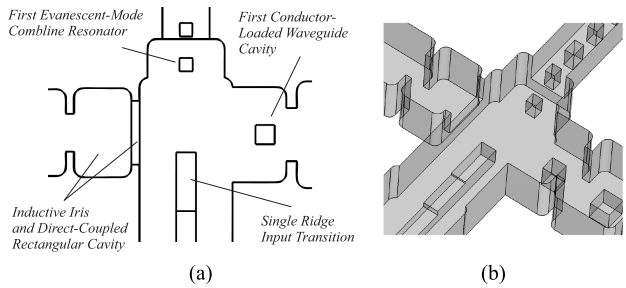

FIGURE 7. A close-up view of the star junction in its (a) outline form and, (b) vacuum-shell form.

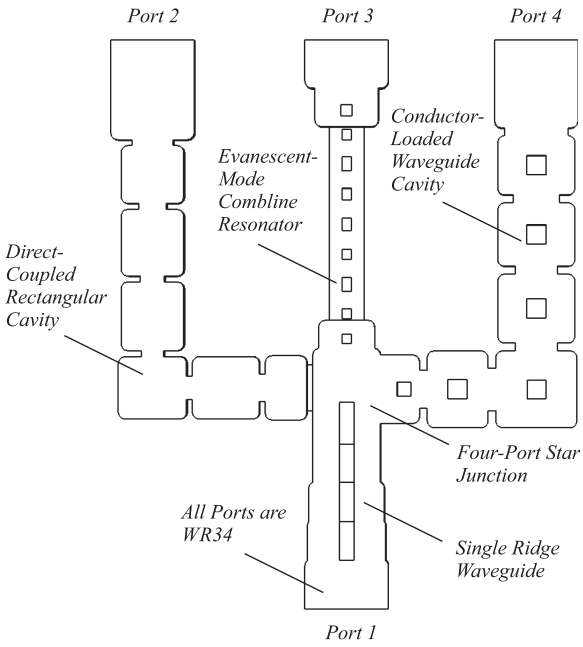

FIGURE 8. Outline of the wideband multiplexer design with use of various filter types.

The following outlines each of the three filter branches' operational specifications and the technology requirements:

- *Filter for Branch 1* - The first filter branch is specified from Port 1 to Port 2 and built up of six direct-coupled rectangular cavities starting from the left-hand side of the star junction. This filter serves the uppermost passband in the system and has been specified with an equiripple bandwidth from 29.5 GHz to 30.5 GHz, for an operational FBW of 1.67% between 29.75 GHz to 30.25 GHz. Rectangular resonator cavities were selected in order obtain the narrow/moderate bandwidth in the upper *Ka*-band while satisfying a filter implementation with a reasonable unloaded Q. In addition, this implementation allows for a cutoff frequency (near the lower range) that can facilitate the use of the two lower frequency passbands in the system without any risk of interference. The upper rejection characteristics will be required to meet the upper spurious-mode conditions that are subject to the next two (lower frequency) filter branches and Table 1.
- *Filter Branch 2* - The second filter branch is specified from Port 1 to Port 3 and built up of nine evanescent-mode combline resonators starting from the inline face of the star junction. This filter serves the center passband in the system and has been specified with an equiripple bandwidth from 23.5 GHz to 27.5 GHz, for an operational FBW of 13.73% between 23.75 GHz to 27.25 GHz. Evanescent-mode posts were selected in order obtain the wide passband in the lower region of the *Ka*-band and allows for a high selectivity and moderate rejection region that would not interfere with the uppermost passband. Due to the large filter passband, the inherent lower unloaded Q of this resonator type is acceptable to accommodate the low insertion loss demands.
- *Filter Branch 3* - The final filter branch is specified from Port 1 to Port 4 and built up of six conductor-loaded cavities starting from the right-hand side of the star junction. This filter serves the lower passband in the system and has been specified with an equiripple bandwidth from 19.5 GHz to 21.25 GHz, for an operational FBW of 6.14% between 19.75 GHz to 21.0 GHz. This moderate FBW is selected for the Satcom downlink and allows for additional information bandwidth from payload applications. For this particular design, emphasis has been focused on compromising reasonable unloaded cavity Q and the required control of spurious cavity modes to satisfy the far out-of-band rejection up to the specified end of the *Ka*-band (>60 dB rejection at 33 GHz). Additionally, specifying the lowest filter branch in this manner, a wide spurious free region could be provided as a way of mitigating any interference with the two uppermost passbands. A general view of this behavior can be observed while studying the single resonator types provided in Fig. 3 and Fig. 4, and extrapolated to meet the final rejection requirements specified in Table 1.

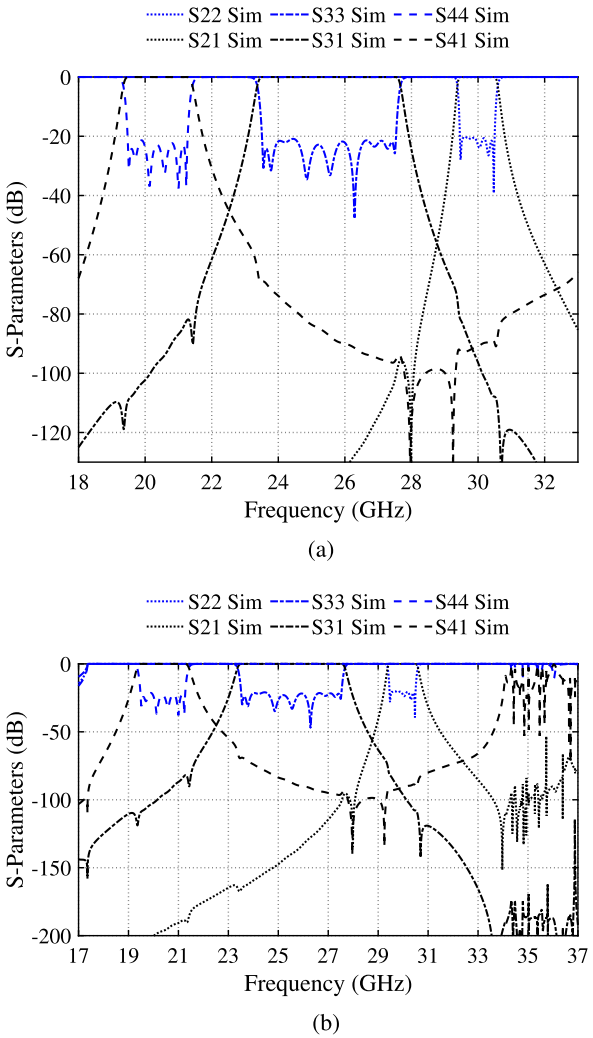

FIGURE 9. (a) Simulated S-parameter results of the multiplexer as proposed in Fig. 2 and further outlined in Fig. 8, and (b) details of the lower frequency cutoff and higher frequency spurious modes of the simulated S-parameter results.

III. WIDEBAND INPUT TRANSITION AND FOUR-PORT JUNCTION

At the core of the multiplexer, a four-port star junction has been developed that enables each of the different waveguide types to interface for the splitting and combining of the signals. A narrow channel width is selected in order to deter spurious and higher order modes from forming in this region while still providing a suitable cutoff frequency for the inclusion of the lowest passband frequencies. In order to feed the narrow four-port junction, the input (common) port is fed by a single-ridge waveguide to standard rectangular waveguide transition. This transition is created to interface with the WR34 input port and selected for its ability to provide good return loss over a wide range of frequencies. Fig. 6 provides the simulated S-parameters of the transition throughout the 18 GHz to 33 GHz region before it is added as the interface to the rest of the star-junction body. The three

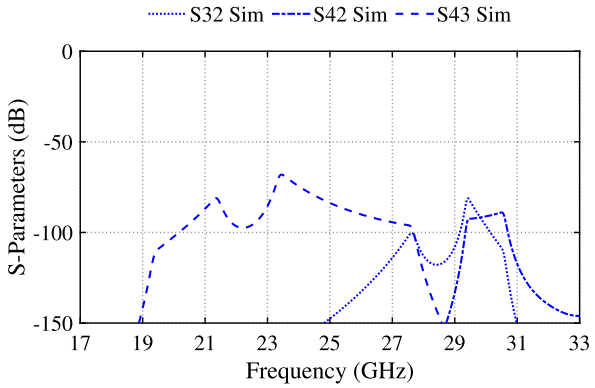

FIGURE 10. Simulated isolation between the filter-branch ports.

output ports (2 through 4) of the star junction are formulated with the following corresponding waveguide filter types, that being: An inductive coupling iris feeding the standard rectangular cavity branch, an evanescent-mode post to feed the evanescent-mode branch, and a single-ridge post to feed the single-ridge (conductor loaded) cavity branch. A close-up view of the star junction in its outline form and vacuum-shell form are provided in Fig. 7.

IV. MODELLING AND SIMULATIONS

A vacuum-shell model of the proposed multiplexer has been provided in Fig. 2 along with its corresponding topology in Fig. 1 while details of the single-ridge input transition and interconnecting star junction are provided in Fig. 6 and Fig. 7, respectively. For a planar view, a detailed outline of the multiplexer model is provided in Fig. 8 and corresponds to each of the filtering branch bullet points outlined in Section II, as well as the single-ridge input transition and four-port junction outlined in Section III.

The simulated S-parameters of this design are shown in Fig. 9(a) for operation between 18 GHz to 33 GHz with each of the specified FBWs mentioned previously. Each of the passbands is designed with better than 20 dB return loss, while the guardband regions reach below 40 dB at the transmission crossovers between each of the passbands. Additionally, it can be noted that the upper rejection of the lowest passband remains spurious free up to the end of the frequency band (i.e., >60 dB up to 33 GHz). Fig. 9(b) is provided as a wideband view of the lowest cutoff frequency and the upper spurious-mode response and plotted over the range of 17 GHz to 37 GHz. The isolation between each of the filter ports is given in Fig. 10 where the lowest isolation is approximately 68.0 dB at 23.45 GHz, and rises to more than 80 dB throughout the rest of the specified frequency range. A close-up view of the simulated insertion loss values while considering an effective conductivity of 15.6 MS/m are provided later in Fig. 14 of Section VI, where the simulated and measured results are compared in detail. Details of the electric-field distribution throughout the structure are provided in Fig. 11 and allow for the reader to understand the interactions of each branch with the interconnecting star junction.

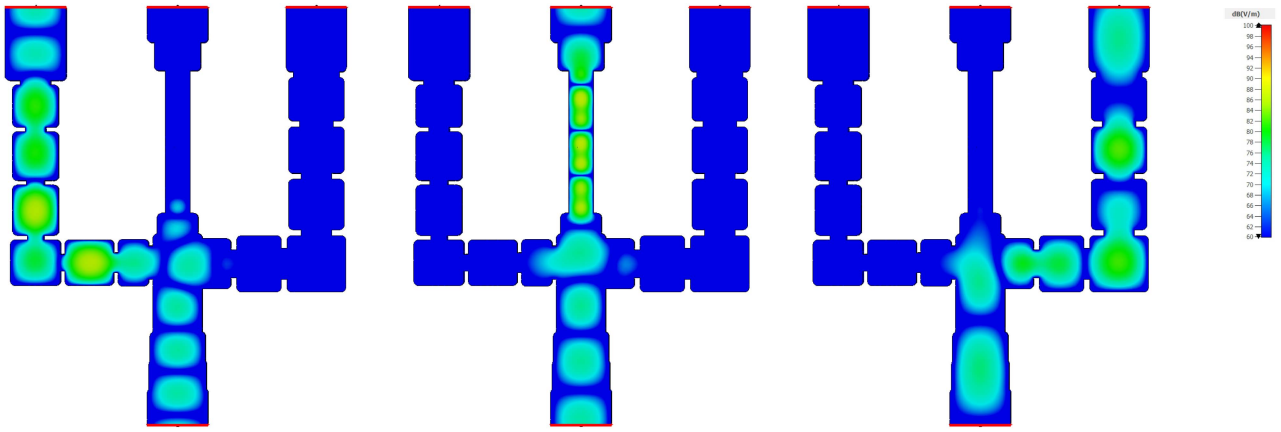

FIGURE 11. **(a) Simulated electric-field distribution through each of the filter branches. (a) Branch 1; the direct coupled cavity section, (b) Branch 2; the evanescent combline section, and (c) Branch 3; the conductor-loaded cavity section.**

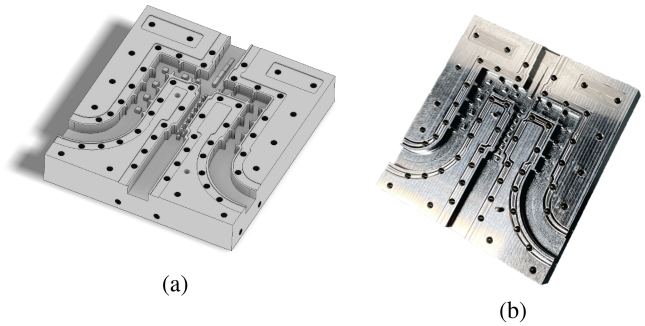

FIGURE 12. **(a) Perspective view of the proposed multiplexer's inner channels and housing in CAD form, and (b) the fabricated multiplexer prototype in aluminum (no metallization is applied).**

V. FABRICATION

For the fabrication of the multiplexer, aluminum has been selected as the cutting material and high-precision CNC milled into two blocks; one for the internal cavities and structures and the other as a cover lid. The advantage of using single ridge waveguide rather than dual ridge can be noted here: milling of the cavities is bound to only one aluminum block and there is no concern for misalignment of the dual ridge sections. All of the corner radii are specified as 0.7 mm. Compression flanges have been added to the outline of the internal channels for efficient pressure contact when the lid is mounted. A simulated CAD model is provided in Fig. 12(a), while the synonymous part is shown as the realized aluminum prototype in Fig. 12(b). For ease of measurement, optional 90-degree H-plane bends were added to the outputs of Port 2 and Port 4, while Port 1 and Port 3 remained inline. The final dimensions of the milled unit are $79 \times 88 \times 23$ mm^3 with a weight of 414 g. The unit has been retained in its aluminum form for measurement and no passivation layer has been applied. Furthermore, no post tuning has been applied.

VI. MEASUREMENT

The multiplexer has been tested using a two-port method with a Rohde & Schwarz ZVA67 network analyzer. The input and *i*th channel are measured, while consequently, the other channel ports are terminated with matched loads. A comparison of the simulated and measured results are presented in Fig. 13(a)–(c) over 18 GHz to 33 GHz, where 22 GHz is the typical lower bound operation of WR34 components. These measurements can be seen to follow each of the three measured passbands closely and exhibit highly accurate results. The measured return loss in all three passbands is better than 19.2 dB. The measured insertion losses taken in the designated operational passband bandwidths are in the range of 0.29 dB to 0.38 dB, 0.38 dB to 0.59 dB, and 0.52 dB to 0.68 dB for the lower, middle and upper passbands, respectively.

Furthermore, it can be shown in Fig. 13(a)–(c), that the rejection characteristics of each passband meet their specified requirements from Table 1. These requirements consist of the 30 dB guardbands spanning 0.5 GHz between each of the adjacent passbands, as well as the more stringent rejection levels of 60 dB that are placed further from the given passbands to suppress out-of-band interference. These rejection requirements are indicated by the green boundary lines. Only a minor offset with regards to the center frequencies of the passbands can be observed. A close-up view of the simulated versus measured insertion losses are provided in Fig. 14 over the full range. The measured isolation between each of the three channels is provided in Fig. 15 and demonstrates an isolation that is better than 68.0 dB for all three channels. In light of the accurate measurements, all of the specifications for the multiplexer have been met. Table 3 is provided as a summary of the electrical and physical measurements. For comparison to manufactured designs that are presented in the literature, Table 4 is provided as an overview of other waveguide-based triplexer designs ranging from 1 GHz up to 220 GHz. It can be noted that the operational bandwidth (MUX FBW = 42%)

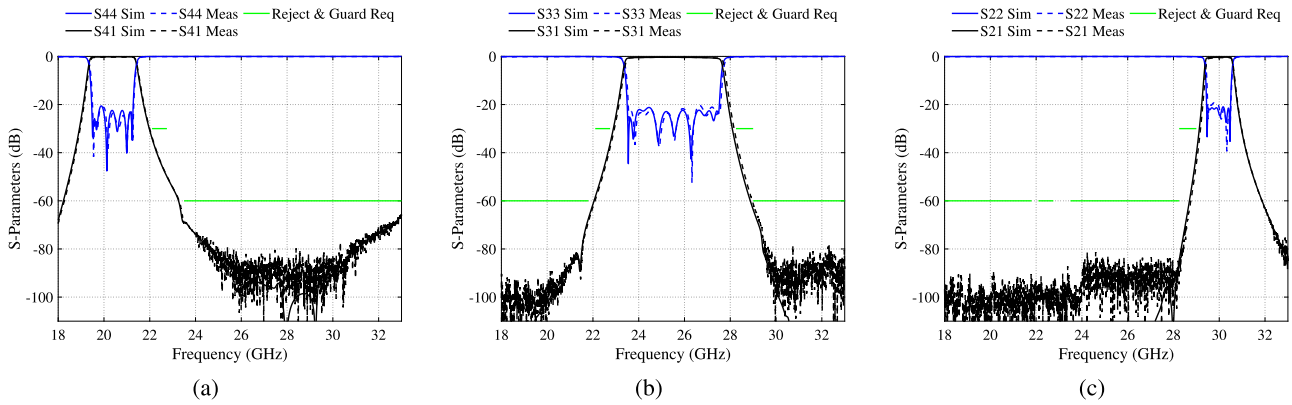

FIGURE 13. (a) Simulated versus measured S-parameter results of the multiplexer. (a) the conductor-loaded cavity section, (b) the combline section, and (c) the direct coupled cavity section. Rejection and guardband requirements are indicated by the green boundary lines. Effective conductivity is taken as 15.6 MS/m.

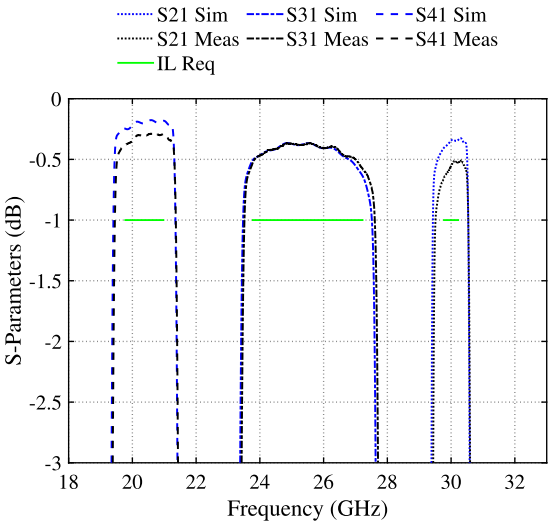

FIGURE 14. Close up view of the simulated versus measured insertion losses for each of the multiplexer branches. Insertion loss requirements are indicated by the green boundary lines. Effective conductivity is taken as 15.6 MS/m.

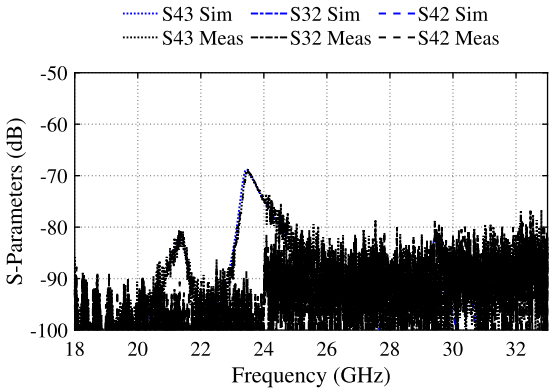

FIGURE 15. Simulated versus measured isolation between the filter branch ports. Effective conductivity is taken as 15.6 MS/m.

TABLE 3 Fabricated *K/Ka*-Band Multiplexer - Electrical and Physical Measurements

	Satcom (Downlink)	Satcom (Uplink)	5/6G
Operational Band [GHz]	19.75 to 21.0	29.75 to 30.25	23.75 to 27.25
Insertion Loss [dB]	0.29 - 0.38	0.52 - 0.68	0.38 - 0.59
Return Loss [dB]	>21	>19.2	>20.3
Rejection / Guard [dB]			
18.0 to 21.25 GHz	-	60	60
22.25 to 22.75 GHz	30	60	30
23.5 to 27.5 GHz	60	60	-
28.25 to 28.75 GHz	60	30	30
29.75 to 33.0 GHz	60	-	60
Size [mm^3]	prototype = (79 x 88 x 23), est.* = (56 x 52 x 8)		
Mass [g]	prototype = 414, est.* = <60		

*Estimated size and weight for final production without requirements for flange interface and bulk prototype size.

of this design is far larger than any other reported designs to date. Furthermore, excellent isolation characteristics are achieved without the need of transmission zero producing topologies.

VII. FUTURE APPLICATIONS

Application of the proposed wideband multiplexer concept can be extended to leading industrial applications for Satcom/terrestrial communications as proposed in [1] and [41]. Modification of the proposed multiplexer model allows for the industry specified bands to be achieved within a similar profile and are exemplified by the transmission simulations provided in Fig. 16(a)–(c) for operational passbands between 19.7 GHz to 20.2 GHz, 24.25 GHz to 27.5 GHz, and 29.5 GHz to 30 GHz with specified guardband and rejection requirements indicated by the green boundary lines. As shown in Fig. 16(a), one of most challenging requirements is to provide a 60 dB rejection up to 35 GHz, however, this condition was successfully met by using the conductor-loaded cavity approach as outlined in Section II. In fact, the simulations are even shown to allow for more than 100 dB rejection in

TABLE 4 Sample Comparison of Manufactured Multiplexers‡ (Waveguide-Based Triplexers Between 1 GHz–220 GHz)

Technol.	Oper. Band (GHz)	MUX FBW (%)	Ch. FBW (%)	TZs	IL* (dB)	RL* (dB)	Isolation (dB)	Layout	Ref.
CNC	11.351 - 13.85	19.8	1.75 / 1.60 / 1.45	No	0.4 / 05 / 0.6	>27	>60	Power div.	[35]
CNC	12.95 - 18.4	34.8	2.3 / 5.3 / 1.64	No	<0.3 / <0.3 / <0.3	>23	>60	**Power div.	[36]
CNC	125 - 156	22.1	5.4 / 5 / 4.6	Yes	0.54 / 0.62 / 0.55	>17	>45	Manifold	[37]
CNC	94.2 - 95.8	1.68	0.53 / 0.42 / 0.52	No	1.5 / 1.5 / 1.5	>10	NA	Manifold	[38]
CNC	210 - 220	4.65	0.95 / 0.93 / 0.91	No	<3 / <3 / <3	>10	NA	Manifold	[39]
CNC	9.7 - 10.3	6.0	1.0 / 1.0 / 0.98	No	0.96 / 1.33 / 1.31	>16	>20	Res. Manifold	[40]
CNC	19.75 - 30.25	42	6.13 / 13.72 / 1.67	No	0.29 / 0.38 / 0.52	>19.2	>68	Star Junct.	T.W.

‡Table values are estimated as best as possible for the presented measured data where not directly reported. *Measured data is reported as the achieved typical value, minimum achieved value, or at center frequency (rather than a range), **Modified E-plane power divider, *Measured data is reported as channel return loss or common port return loss. TZs = Transmission zeros, NA = Not available.

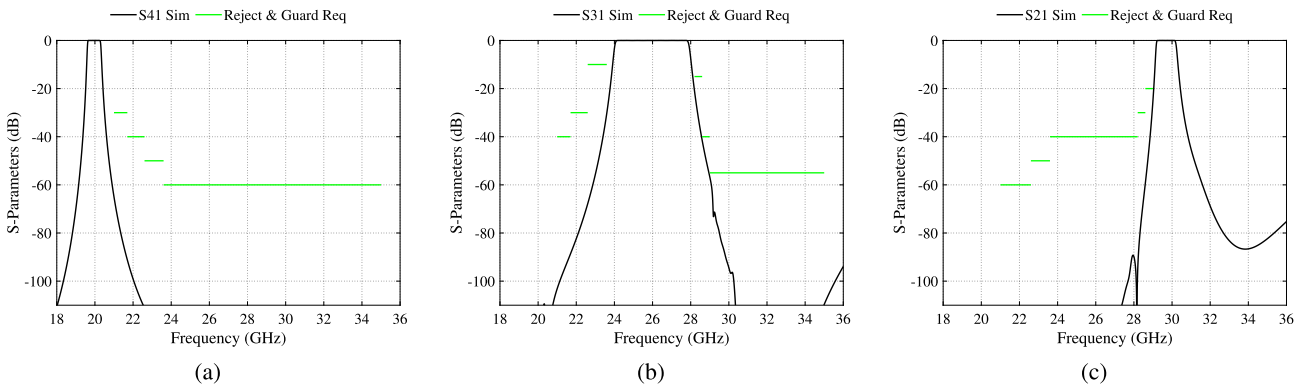

FIGURE 16. Simulated theoretical insertion loss results for an industry initiated multiplexer mask as proposed in [1] and [41]. Rejection requirements are indicated by the green boundary lines.

this region by utilizing this method. In this manner, an implementation of the general design approach, as well as the realizable hardware, can be applied to the next-generation of integrated terminals with HTSs utilizing FDD, and 5G/6G mmWave eMBB utilizing TDD.

VIII. CONCLUSION AND OUTLOOK

In this work, a novel wideband multiplexer concept for multi-use Satcom/terrestrial applications has been proposed and demonstrated for multi-band use. Using an array of RF filtering techniques, three wideband channels are demonstrated for passband operation over a frequency range of 19.5 GHz to 30.5 GHz. The broad frequency range of these channels are combined through the use of a four-port star junction that is fed from a single ridge-waveguide transformer. For the verification of the approach a stand-alone multiplexer unit has been designed considering standard WR34 waveguide flange interfaces at all of the input/output ports. The measured results are demonstrated to be highly accurate when compared with the analyzed characteristics of the model and, thus, demonstrate the validation of the general approach.

The size of the realized multiplexer for verification purposes is mainly driven by the use of standard WR34 flange interfaces (prototype size: 79 × 88 × 23 mm). This design is already compact, however, for an application in integrated equipment solutions, there is no need of standard waveguide-flange style interfacing with the dedicated units (e.g., transmit amplifier, LNA,. . .). Such units allow direct interconnections with associated transitions to facilitate overall compact equipment designs. Consequently, the multiplexer design is well suited for integrated equipment solutions, e.g., it can be considered for a combined implementation with the transmit and receive amplifiers in a common housing with the appropriate transitions for the direct interconnections of the units. This will be an essential prerequisite for overall high-performance and low-cost implementations of multiple-use communications terminals.

As demonstrated, the concept is suitable for future requirements proposed by industry. The straight-forward design profile does not require the use of cross-couplings or frequency-dependent inverters for generating transmission-zeros to meet any of the rejection or isolation requirements. This is due to the utilization of the high selectivity provided by each of the all-pole filter designs combined with the clever use of each specific resonator type to maintain spurious-free regions above each sequential passband. This work provides an innovative multi-resonator type solution for overcoming the stringent demands of wideband multiplexers and can be applied for practical multi-use Satcom/terrestrial terminals in the future.

REFERENCES

[1] F. De Paolis, "Satellite filters for 5G/6G and beyond," in *Proc. IEEE MTT-S Int. Microw. Filter Workshop*, 2021, pp. 148–150, doi: 10.1109/IMFW49589.2021.9642277.

[2] S. Cioni, R. De Gaudenzi, O. Del Rio Herrero, and N. Girault, "On the satellite role in the era of 5G massive machine type communications," *IEEE Netw.*, vol. 32, no. 5, pp. 54–61, Sep./Oct. 2018, doi: 10.1109/MNET.2018.1800024.

[3] R. De Gaudenzi, P. Angeletti, D. Petrolati, and E. Re, "Future technologies for very high throughput satellite systems," *Int. J. Sat. Comm. Netw.*, vol. 38, no. 2, pp. 141–161, 2020, doi: 10.1002/SAT.1327.

[4] A. Sheikhi, S. M. Razavizadeh, and I. Lee, "A comparison of TDD and FDD massive MIMO systems against smart jamming," *IEEE Access*, vol. 8, pp. 72068–72077, 2020, doi: 10.1109/ACCESS.2020.2987606.

[5] M. K. Emara and S. Gupta, "Integrated multiport leaky-wave antenna multiplexer/demultiplexer system for millimeter-wave communication," *IEEE Trans. Antennas Propag.*, vol. 69, no. 9, pp. 5244–5256, Sep. 2021, doi: 10.1109/TAP.2021.3060138.

[6] J. D. Rhodes and R. Levy, "A generalized multiplexer theory," *IEEE Trans. Microw. Theory Techn.*, vol. 27, no. 2, pp. 99–111, Feb. 1979, doi: 10.1109/TMTT.1979.1129570.

[7] J. D. Rhodes and R. Levy, "Design of general manifold multiplexers," *IEEE Trans. Microw. Theory Techn.*, vol. 27, no. 2, pp. 111–123, Feb. 1979, doi: 10.1109/TMTT.1979.1129571.

[8] G. Macchiarella, "Synthesis of star-junction multiplexers," *IEEE Microw. Mag.*, vol. 12, no. 6, pp. 101–109, Oct. 2011, doi: 10.1109/MMM.2011.942011.

[9] G. Macchiarella and S. Tamiazzo, "Synthesis of star-junction multiplexers," *IEEE Trans Microw. Theory Techn.*, vol. 58, no. 12, pp. 3732–3741, Dec. 2010, doi: 10.1109/TMTT.2010.2086570.

[10] J. Uher, J. Bornemann, and U. Rosenberg, *Waveguide Components for Antenna Feed Systems: Theory and CAD*. Norwood, MA, USA: Artech House Antenna Library, 1993.

[11] R. J. Cameron, C. M. Kudsia, and R. R. Mansour, *Microwave Filters for Communication Systems: Fundamentals, Design, and Applications*. Hoboken, NJ, USA: Wiley, 2018.

[12] G. L. Matthaei, L. Young, and E. M. Jones, *Microwave Filters, Impedance-Matching Networks, and Coupling Structures*. Norwood, MA, USA: Artech House, 1980.

[13] Z. Tan, Q.-Y. Zhang, Y.-L. Lei, Y. Zhao, and J.-Q. Ding, "Terahertz waveguide multiplexers: A review," *Microw. Opt. Technol. Lett.*, vol. 65, no. 7, pp. 1925–1935, doi: 10.1002/MOP.33653.

[14] K. Zhou and K. Wu, "Substrate integrated waveguide multiband bandpass filters and multiplexers: Current status and future outlook," *IEEE J. Microwaves*, vol. 3, no. 1, pp. 466–483, Jan. 2023, doi: 10.1109/JMW.2022.3227131.

[15] R. V. Snyder, A. Mortazawi, I. Hunter, S. Bastioli, G. Macchiarella, and K. Wu, "Present and future trends in filters and multiplexers," *IEEE Trans. Microw. Theory Techn.*, vol. 63, no. 10, pp. 3324–3360, Oct. 2015, doi: 10.1109/TMTT.2015.2475245.

[16] F. Teberio, I. Arregui, P. Soto, M. A. G. Laso, V. E. Boria, and M. Guglielmi, "High-performance compact diplexers for Ku/K-band satellite applications," *IEEE Trans. Microw. Theory Techn.*, vol. 65, no. 10, pp. 3866–3876, Oct. 2017, doi: 10.1109/TMTT.2017.2691773.

[17] F. Teberio et al., "Compact broadband waveguide diplexer for satellite applications," in *Proc. IEEE MTT-S Int. Microw. Symp.*, 2016, pp. 1–4, doi: 10.1109/MWSYM.2016.7540231.

[18] U. Rosenberg, K. Beis, U. Mahr, and W. Speldrich, "Emerging high performance wide band feed systems for multiaccess of satellite and earth station antennas," in *Proc. 14th AIAA Int. Commun. Sat. Syst. Conf.*, 1992, pp. 711–718, doi: 10.2514/6.1992-1904.

[19] Q. You, Y. Lu, Y. Wang, J. Xu, J. Huang, and W. Hong, "Hollow-waveguide tri-band shared-aperture full-corporate-feed continuous transverse stub antenna," *IEEE Trans. Antennas Propag.*, vol. 70, no. 8, pp. 6635–6645, Aug. 2022, doi: 10.1109/TAP.2022.3161265.

[20] U. Rosenberg, "Fully integrated waveguide subsystem approach facilitates low cost transceiver equipment designs," in *Proc. 7th Int. Workshop Microw. Filters*, 2014, pp. 1–8.

[21] U. Rosenberg, J. Ebinger, and S. Amari, "Advanced receive/transmit diplexer design for emerging mm-wave access radio applications," in *Proc. IEEE MTT-S Int. Microw. Symp.*, 2006, pp. 1217–1220, doi: 10.1109/MWSYM.2006.249429.

[22] U. Rosenberg, M. Knipp, and S. Amari, "Compact diplexer design using different e-plane triplets to serve contiguous passbands with high interband selectivity," in *Proc. Eur. Microw. Conf.*, 2006, pp. 133–136, doi: 10.1109/EUMC.2006.281218.

[23] C. Bartlett, O. Glubokov, F. Kamrath, and M. Höft, "Highly selective broadband mm-wave diplexer design," *IEEE Microw. Wireless Technol. Lett.*, vol. 33, no. 2, pp. 149–152, Feb. 2023, doi: 10.1109/LMWC.2022.3205425.

[24] S. Cogollos et al., "Efficient design of waveguide manifold multiplexers based on low-order EM distributed models," *IEEE Trans. Microw. Theory Techn.*, vol. 63, no. 8, pp. 2540–2549, Aug. 2015, doi: 10.1109/TMTT.2015.2442990.

[25] P. Zhao and K.-L. Wu, "An iterative and analytical approach to optimal synthesis of a multiplexer with a star-junction," *IEEE Trans. Microw. Theory Techn.*, vol. 62, no. 12, pp. 3362–3369, Dec. 2014, doi: 10.1109/TMTT.2014.2364222.

[26] M. M. Mendoza, M. G. Tudela, and R. G.-C. Camuñas, "Design of a four channel C-band multiplexer with a modified star-junction topology," in *Proc. IEEE/MTT-S Int. Microw. Symp.*, 2020, pp. 587–590, doi: 10.1109/IMS30576.2020.9224067.

[27] H. Hu, K.-L. Wu, and R. J. Cameron, "Stepped circular waveguide dual-mode filters for broadband contiguous multiplexers," *IEEE Trans. Microw. Theory Techn.*, vol. 61, no. 1, pp. 139–145, Jan. 2013, doi: 10.1109/TMTT.2012.2227787.

[28] A. Pons Abenza, M. Martinez-Mendoza, F. D. Quesada Pereira, and A. Alvarez-Melcon, "Design of manifold multiplexers in all-inductive dual-mode rectangular waveguide technology using the coupling matrix formalism," *Radio Sci.*, vol. 51, no. 7, pp. 1065–1080, 2016, doi: 10.1002/2016RS005999.

[29] V. Nocella et al., "E-band cavity diplexer based on micromachined technology," *Int. J. Microw. Wireless Technol.*, vol. 8, no. 2, pp. 179–184, 2016, doi: 10.1017/S175907871400155X.

[30] C. Rauscher, S. W. Kirchoefer, J. M. Pond, A. C. Guyette, and D. R. Jachowski, "A compact ridge-waveguide contiguous-channel frequency multiplexer," *IEEE Trans. Microw. Theory Techn.*, vol. 57, no. 3, pp. 647–656, Mar. 2009, doi: 10.1109/TMTT.2009.2013288.

[31] C. Bartlett, J. Bornemann, and M. Höft, "3D-printing and high-precision milling of w-band filter components with admittance inverter sequences," *IEEE Trans. Compon., Packag. Manuf. Technol.*, vol. 11, no. 12, pp. 2140–2147, Dec. 2021, doi: 10.1109/TCPMT.2021.3116220.

[32] Y. Feng et al., "A 200–225-GHz manifold-coupled multiplexer utilizing metal waveguides," *IEEE Trans. Microw. Theory Techn.*, vol. 69, no. 12, pp. 5327–5333, Dec. 2021, doi: 10.1109/TMTT.2021.3119316.

[33] D. Tiradossi et al., "Micromachined on silicon miniaturized Ka-band diplexer for ground-segment user terminals," in *Proc. IEEE 52nd Eur. Microw. Conf.*, 2022, pp. 119–122, doi: 10.23919/EuMC54642.2022.9924289.

[34] U. Rosenberg, A. Bradt, M. Perelshtein, and P. Bourbonnais, "Extreme broadband waveguide diplexer design for high performance antenna feed systems," in *Proc. IEEE 40th Eur. Microw. Conf.*, 2010, pp. 1249–1252, doi: 10.23919/EUMC.2010.5616721.

[35] L. Accatino, B. Piovano, G. Vercellino, and R. Ravanelli, "Design and breadboarding of a compact and tuningless triplexer for satellite applications," in *Proc. IEEE Antennas Propag. Soc. Int. Symp.*, 1997, pp. 1418–1421, doi: 10.1109/APS.1997.631863.

[36] J. Ruiz-Cruz, J. R. Montejo-Garai, J. M. Rebollar, and S. Sobrino, "Compact full ku-band triplexer with improved e-plane power divider," *Prog. Electromagn. Res.*, vol. 86, pp. 39–51, 2008, doi: 10.2528/PIER08082803.

[37] Y. Feng, B. Zhang, Y. Liu, Z. Niu, Y. Fan, and X. Chen, "A D-band manifold triplexer with high isolation utilizing novel waveguide dual-mode filters," *IEEE Trans. THz Sci. Technol.*, vol. 12, no. 6, pp. 678–681, Nov. 2022, doi: 10.1109/TTHZ.2022.3203308.

[38] A. Morini, G. Venanzoni, M. Farina, and T. Rozzi, "Practical design of a high-power tuning-less w-band triplexer for ground radar surveillance systems," *IET Microw., Antennas Propag.*, vol. 1, no. 4, pp. 882–826, 2007, doi: 10.1049/iet-map:20070020.

[39] Y. Feng, B. Zhang, B. Dai, and F. Shen, "Design and performance of a 210-220 GHz manifold triplexer," in *Proc. IEEE 46th Int. Conf. Infrared Millimeter THz Waves*, 2021, pp. 1–2, doi: 10.1109/IRMMW-THz50926.2021.9567110.

[40] Y. Yu, Y. Wang, C. Guo, Q. S. Cheng, and M. Yu, "Resonant manifold multiplexers," *IEEE Trans. Microw. Theory Techn.*, vol. 70, no. 2, pp. 1059–1071, Feb. 2022, doi: 10.1109/TMTT.2021.3120450.

[41] European Space Agency (ESA), "Space for 5G & 6G," Jul. 2023, [Online]. Available: https://artes.esa.int/opportunity-integrated-wideband-multiplexer-hybrid-satcomterrestrial-5g-user-terminals

CHAD BARTLETT (Member, IEEE) was born in Nelson, BC, Canada, in 1987. He received the B.Eng. and MA.Sc. degrees in electrical and computer engineering from the University of Victoria, Victoria, BC, Canada, in 2017 and 2019, respectively, and the Dr.-Ing. degree in electrical and information engineering from Kiel University, Kiel, Germany, in 2023. From 2019 to 2023, he was a Member of the European Union's Horizon 2020 research and innovation program for early-stage researchers where his work focused on advanced filter solutions for high-performance millimetre and submillimetre-wave systems. His primary research interests include microwave and millimetre-wave passive components, filters, multiplexers and antenna networks for the next generation of satellite and communication systems, as well as developing methods for overcoming challenges in microscale designs.

MICHAEL HÖFT (Senior Member, IEEE) was born in Lübeck, Germany, in 1972. He received the Dipl.-Ing. degree in electrical engineering and the Dr.-Ing. degree from Hamburg University of Technology, Hamburg, Germany, in 1997 and 2002, respectively. From 2002 to 2013, he was with the Communications Laboratory, European Technology Center, Panasonic Industrial Devices Europe GmbH, Lüneburg. He was a Research Engineer and then the Team Leader, where he had been engaged in research and development of microwave circuitry and components, particularly filters for cellular radio communications. From 2010 to 2013, he was the Group Leader of research and development of sensor and network devices. Since 2013, he has been a Full Professor with the Faculty of Engineering, University of Kiel, Kiel, Germany, where he currently heads the Chair of Microwave Engineering, Institute of Electrical and Information Engineering. His research interests include active and passive microwave components, submillimeter-wave quasioptical techniques and circuitry, microwave and field measurement techniques, microwave filters, microwave sensors, and magnetic field sensors. Dr. Höft is a Member of the European Microwave Association, the Association of German Engineers, and German Institute of Electrical Engineers.

UWE ROSENBERG (Life Senior Member, IEEE) has been with several international companies where he has been responsible for the research, development and design of advanced passive microwave subsystems and components for communications, remote sensing, navigation and other systems since 1985. The related equipment developments have been dedicated to a variety of applications, like satellites, large earth stations, trunk and access radio, and mobile base stations. During this time he was in charge of numerous developments of novel filter, multiplexer, coupler, feed system and waveguide solutions considering high RF performance, convenient production technologies, and suitable equipment integrations while focusing on overall low equipment cost. He is the Managing Director of Mician Global Engineering GbR, Bremen, Germany, which he co-founded together with partners and he is providing consultancy services for international companies. He has coauthored *Waveguide Components for Antenna Feed Systems: Theory and CAD* (Artech House, 1993). He has also authored or coauthored more than 110 technical papers and has originated more than 50 granted microwave design patents.